

Broccoli Sprouts Delay Prostate Cancer Formation and Decrease Prostate Cancer Severity with a Concurrent Decrease in HDAC3 Protein Expression in Transgenic Adenocarcinoma of the Mouse Prostate (TRAMP) Mice

Laura M Beaver,^{1,2} Christiane V Lohr,^{2,3} John D Clarke,^{1,2} Sarah T Glasser,¹ Greg W Watson,^{1,2} Carmen P Wong,^{1,2} Zhenzhen Zhang,⁶ David E Williams,^{2,4} Roderick H Dashwood,^{2,4} Jackilen Shannon,⁴ Philippe Thuillier,^{6,7} and Emily Ho^{1,2,5}

¹School of Biological and Population Health Sciences; ²Linus Pauling Institute; and ³Department of Biomedical Sciences, College of Veterinary Medicine; ⁴Department of Environmental and Molecular Toxicology, College of Agricultural Sciences; and ⁵Moore Family Center for Whole Grain Foods, Nutrition and Preventive Health, Oregon State University, Corvallis, OR; and ⁶OHSU-PSU School of Public Health, and ⁷Department of Dermatology, Oregon Health & Science University, Portland, OR

Abstract

Background: Cruciferous vegetables have been associated with the chemoprevention of cancer. Epigenetic regulators have been identified as important targets for prostate cancer chemoprevention. Treatment of human prostate cancer cells with sulforaphane (SFN), a chemical from broccoli and broccoli sprouts, inhibits epigenetic regulators such as histone deacetylase (HDAC) enzymes, but it is not known whether consumption of a diet high in broccoli sprouts impacts epigenetic mechanisms in an in vivo model of prostate cancer.

Objective: In the transgenic adenocarcinoma of the mouse prostate (TRAMP) model, we tested the hypothesis that a broccoli sprout diet suppresses prostate cancer, inhibits HDAC expression, alters histone modifications, and changes the expression of genes regulated by HDACs.

Methods: TRAMP mice were fed a 15% broccoli sprout or control AIN93G diet; tissue samples were collected at 12 and 28 wk of age.

Results: Mice fed broccoli sprouts had detectable amounts of SFN metabolites in liver, kidney, colon, and prostate tissues. Broccoli sprouts reduced prostate cancer incidence and progression to invasive cancer by 11- and 2.4-fold at 12 and 28 wk of age, respectively. There was a significant decline in HDAC3 protein expression in the epithelial cells of prostate ventral and anterior lobes at age 12 wk. Broccoli sprout consumption also decreased histone H3 lysine 9 trimethylation in the ventral lobe (age 12 wk), and decreased histone H3 lysine 18 acetylation in all prostate lobes (age 28 wk). A decline in *p16* mRNA levels, a gene regulated by HDAC3, was associated with broccoli sprout consumption, but no significant changes were noted at the protein level.

Conclusions: Broccoli sprout intake was associated with a decline in prostate cancer occurrence and HDAC3 protein expression in the prostate, extending prior work that implicated loss of HDAC3/ corepressor interactions as a key preventive mechanism by SFN in vivo. *Curr Dev Nutr* 2018;2:nzy002.

Introduction

Prostate cancer is the second most frequently diagnosed cancer among men globally, and is a leading cause of cancer-related deaths in the United States (1, 2). The disease is typically slow growing, and although abnormalities in the prostate epithelium can be observed in men in their twenties or thirties, prostate cancer generally does not become of clinical concern until later in life (3–5).



Keywords: broccoli, chemoprevention, histone deacetylase (HDAC), histone H3 lysine 18 acetylation (H3K18ac), epigenetics, prostate cancer, TRAMP mouse model, sulforaphane

© 2018, Stamm et al. This is an open access article distributed under the terms of the Creative Commons Attribution Non-Commercial License (<http://creativecommons.org/licenses/by-nc/4.0/>), which permits noncommercial re-use, distribution, and reproduction in any medium, provided the original work is properly cited. For commercial re-use, please contact journals.permissions@oup.com

Manuscript received November 6, 2017. Initial review completed December 21, 2017. Revision accepted December 21, 2017. Published online December 26, 2017.

Supported in part by the Oregon Agricultural Experimental Station, and by the National Cancer Institute (P01 CA090890, R01 CA122959).

Author disclosures: LMB, CVL, JDC, STG, GWW, CPW, ZZ, DEW, RHD, JS, PT, and EH, no conflicts of interest.

Supplemental Table 1 and Figures 1–3 are available from the “Supplementary data” link in the online posting of the article and from the same link in the online table of contents at <https://academic.oup.com/cdn/>.

Present address for JDC: Department of Pharmaceutical Sciences, Washington State University, Spokane, WA.

Present address for RHD: Center for Epigenetics & Disease Prevention, Texas A&M College of Medicine, Houston, TX.

Abbreviations: HDAC, histone deacetylase; H3K, histone H3 lysine; H3K9ac, acetyl-histone H3 lysine 9; H3K9me3, trimethyl-histone H3 lysine 9; H3K18ac, acetyl-histone H3 lysine 18; H&E, hematoxylin and eosin; mPIN, mouse prostatic intraepithelial neoplasia; Nrf2, nuclear factor (erythroid-derived 2)-like 2; OHSU, Oregon Health and Science University; SERPINB5, serpin family B member 5; SFN, sulforaphane; SFN-NAC, sulforaphane-*N*-acetylcysteine; STAT3, signal transducer and activator of transcription 3; TRAMP, transgenic adenocarcinoma of the mouse prostate. Address correspondence to EH (e-mail: emily.ho@oregonstate.edu).

The long latency period of prostate cancer suggests that therapeutic strategies that slow disease progression could be beneficial by delaying full disease onset and possibly decreasing invasive surgical procedures such as prostatectomy. Increasing the latency period of prostate cancer could also be beneficial by increasing the period of time during which a therapeutic intervention could occur. Characterization of the molecular mechanisms that delay prostate cancer formation will be beneficial to facilitate the development of effective chemopreventive strategies.

An association between increased cruciferous vegetable intake and a reduced risk of developing, or being diagnosed with, prostate cancer has been reported (6). Cruciferous vegetables, such as broccoli and broccoli sprouts, are a rich source of glucosinolates (7). When broccoli sprouts are chopped or chewed, the glucosinolate glucoraphanin interacts with the enzyme myrosinase, producing the phytochemical sulforaphane (SFN) (7). Broccoli sprouts and SFN have chemopreventive and cancer-suppressive properties in carcinogen-induced and genetic models of prostate cancer (7–9); however, the mechanisms by which they act *in vivo* are not completely understood. SFN has been shown to inhibit the initiation of cancer by blocking damage caused by carcinogens through the induction of phase 2 enzymes via kelch-like ECH associated protein 1 (Keap1) and nuclear factor (erythroid-derived 2)-like 2 (Nrf2) signaling (10–13). In the transgenic adenocarcinoma of the mouse prostate (TRAMP) model of prostate cancer, broccoli consumption and/or SFN treatment has been shown to slow prostate cancer growth and metastasis (8, 9, 14, 15). Several potential mechanisms have been implicated, including the induction of Nrf2-related pathways, inhibition of the cancer-promoting Akt signaling cascade, suppression of a chemokine receptor (CXCR4), and through augmenting the lytic activity of natural killer cells (8, 9, 14, 15). In contrast to these results, Liu et al. (16) did not find a significant decrease in prostate cancer in TRAMP mice fed a diet high in broccoli sprouts, highlighting a degree of controversy regarding cruciferous vegetable intake and the prevention of prostate cancer.

A hallmark of cancer development is the global modification of epigenetic marks (17). These marks regulate chromatin structure and thus participate in the regulation of gene expression and genome stability. Cancer cells often have dysregulated expression of genes that control epigenetics, such as upregulated histone deacetylase (HDAC) enzymes (18, 19). This contributes to cancer development and progression by turning off tumor suppressor genes, or promoting the expression of oncogenes (20). We and others have shown that SFN can alter epigenetic endpoints in cancer cell lines and tissues, including suppression of HDAC expression, changes in DNA methylation, and increased expression of epigenetically repressed genes such as *p21* and *p16* (21–29). In an *in vitro* study of TRAMP C1 cells, SFN was shown to restore Nrf2 expression through epigenetic modifications and attenuated the expression of several HDAC proteins (13). Although there is substantial evidence that SFN exposure can influence epigenetic endpoints in cancer cells, it has not yet been shown in an *in vivo* model of prostate cancer that consumption of a whole food rich in SFN, such as broccoli sprouts, can induce changes in epigenetic regulators and contribute to chemoprevention. We sought to test the hypothesis that consumption of a diet high in broccoli sprouts suppresses prostate cancer, inhibits HDAC expression, alters histone modifications, and changes expression of genes regulated by HDACs. We show that consumption of a diet high in broccoli sprouts decreased the incidence and severity of

prostate cancer, reduced HDAC3 protein, and altered epigenetic related endpoints.

Methods

Husbandry and study design

Custom AIN93G diet with 15% broccoli sprout powder and matched control diet were prepared by Research Diets (**Supplemental Table 1**). This 15% broccoli sprout diet had 400 mg SFN/kg diet, which was chosen because it is equivalent to 1 mg SFN/d which has been used in previous studies (14, 15, 30). Broccoli sprout powder was purchased from Natural Sprouts Company, LLC. Diets were stored protected from the light at -20°C . Male TRAMP mice in C57BL/6 background were obtained from Jackson Lab and bred in the Oregon Health & Science University (OHSU) animal facility (31–33). Animal protocol was approved by the OHSU Institutional Animal Care and Use Committee. Mice were housed with a 12-h light and 12-h dark cycle, in a temperature- and humidity-controlled environment and fed standard lab chow. At 4 wk of age the mice were placed on either the broccoli sprout or AIN93G control diet. Food consumption was measured over the course of the study and no difference was found in the intake of food between the control and broccoli sprout-fed groups.

Mice were killed in the morning during a 3- to 4-h window at 12 and 28 wk of age. Lung, liver, spleen, kidney, colon, and urogenital tract were removed. The weights of the urogenital tract and prostate lobes were recorded. The prostate lobes were then formalin fixed, paraffin embedded, sectioned, and stained with hematoxylin and eosin (H&E) and scored for cancer incidence and severity by multiple pathologists (CVL from Oregon Veterinary Diagnostic Laboratory at Oregon State University and PT from OHSU). Some prostates were further dissected to separate the anterior, dorsolateral, and ventral lobes and analyzed separately because in this TRAMP model the cancer is driven by the T antigen oncoprotein primarily in the ventral and dorsolateral lobes [reviewed in (34)]. Individual lobes were snap frozen or put into RNA later for subsequent molecular assays.

HPLC-MS/MS analysis

The methods for evaluating amounts of SFN metabolites in mouse tissues via HPLC-MS/MS analysis were performed as previously described (35). Briefly, ~ 50 mg frozen tissue was homogenized using a mortar and pestle in liquid nitrogen. An internal standard [5 μL of 100 μM deuterated SFN-*N*-acetylcysteine (SFN-NAC)] and 50 μL of 10% TFA (v:v) in water was added to the sample and vortexed vigorously. The homogenate was then frozen at -80°C . Later samples were thawed, vortexed, and centrifuged (11,600 $\times g$, 5 min, 4°C), and the supernatant filtered through a 0.2 μm pore size filter. A 10- μL portion of filtered sample was separated on a Shimadzu Prominence HPLC using a reversed-phase Phenomenex Kinetex PFP 2.6 μm 100 \AA 100 \times 2.6 mm HPLC column. The LC eluent was analyzed by an API triple quad mass spectrometer 3200 (Applied Biosystems) with electrospray ionization in positive mode. Tandem MS using multiple reaction monitoring was used to detect the analytes with the following precursor and product ions: SFN (178 > 114), SFN-glutathione (485 > 114), SFN-cysteinylglycine (356 > 114), SFN-cysteine (299 > 114), and SFN-NAC (341 > 114). Spike and recovery experiments using the internal

standard confirmed that >80% of all compounds were recovered. Quantification was performed by using a standard curve ranging from 0.16 to 25 μ M.

Immunohistochemistry

Immunohistochemical staining was performed on an autostainer (Dako Autostainer Universal Staining System) following standard operating procedures of the Oregon Veterinary Diagnostic Laboratory. In brief, paraffin sections were high-temperature antigen retrieved with BDTM Retrieval A solution (Dako), pH 9.0 (HDAC6) or pH 6.0 (all others). Endogenous peroxidase activity was blocked in methanol containing 3% hydrogen peroxide (10 min). Primary rabbit anti-human antibodies for HDAC3 (Abcam ab32369), HDAC6 (Abcam ab1440), acetyl-histone H3 lysine 18 (H3K18ac; Abcam ab1191), histone H3 lysine 9 acetylation (H3K9ac; Cell Signaling 9671), and trimethyl-histone H3 lysine 9 (H3K9me3; Abcam ab8898) were applied for 30 min at room temperature. MaxPoly-One Polymer HRP Rabbit Detection solution (MaxVision Biosciences) was applied (7 min, room temperature). Nova Red (SK-4800; Vector Labs) was used as chromagen and Dako hematoxylin (S3302) as counterstain. Serial sections of neoplastic tissue incubated with Dako Universal negative serum served as negative controls. Images were visualized on a Nikon system that included an Eclipse E400 microscope, DS-Fi2 camera, and NIS-Elements BR software package. For HDAC3, HDAC6, H3K9ac, and H3K9me3, 5 images were captured for each prostate lobe for each individual mouse. HDAC3 and H3K9ac images were taken with 400 \times magnification with a correction for white balance and the mean intensity was calculated by the software for 25 nuclei in each of the images, and then averaged for each individual. HDAC6 images were captured with 200 \times magnification and the intensity of cytoplasmic staining was calculated by the software for 3 regions/image. HDAC6 intensity values in each image were then corrected for differences in white balance, and then averaged for each mouse. For H3K9me3, images were captured with 1000 \times magnification and staining intensity was measured with the software as follows: 1) in punctate regions of the nucleus with high-intensity staining that we refer to as foci; and 2) over the whole nucleus. Each H3K9me3 image had between 20 and 70 nuclei that were fully in focus and quantified. On average, there were ~3 foci of H3K9me3 staining analyzed per nuclei. The staining intensity results were then averaged for each mouse. The number and size of foci with H3K9me3 staining was also captured. The staining intensity data for HDAC3, HDAC6, H3K9ac, and H3K9me3 were expressed as mean staining intensity, subtracted from the intensity of true white, and expressed as a percentage of all possible color. Positive staining for H3K18ac was defined as the intensity of red chromagen precipitate in the nuclei and was scored blindly on a scale from 0 to 3.

Quantitative real-time PCR

Total RNA was collected from indicated prostate lobes in 12- to 13-wk-old mice using a standard Trizol extraction method (Life Technologies). cDNA was synthesized using 1 μ g of total RNA and SuperScript III First-Strand Synthesis SuperMix (Life Technologies). Real-time qPCR was done using primers that amplify all known transcript isoforms of each mouse gene as a single product of expected size, between 140 and 300 bp, with the exception of *p16* where the primers were designed to only amplify *p16* and not the isoform of *CDKN2A* that codes for ARF (alternate open reading frame). Primer sequences were as follows: *18s* (forward) 5'-CCGCAGCTAGGAATAATGGAAT-3' and

(reverse) 5'-CGAACCTCCGACTTTCGTTCT-3'; *CtIP* (also known as RBBP) (forward) 5'-GACCCAGGAGCAGACCTTTC-3' and (reverse) 5'-CATCTGGTACCTGGGAGAAGC-3'; heme oxygenase 1 (HO1) (forward) 5'-GACACCTGAGGTCAAGCACA-3' and (reverse) 5'-CTAGCAGGCCTCTGACGAAG-3'; NAD(P)H dehydrogenase, quinone 1 (NQO1) (forward) 5'-TAGCCTGTAGCCAGCCCTAA-3' and (reverse) 5'-GCCTCCTTCATGGCGTAGTT-3'; *p16* (forward) 5'-AACTCGAGGAGAGCCATCTG-3' and (reverse) 5'-GGGGTACGACCCGAAAGAGTT-3'; serpin family B member 5 (*Serpinb5*) (forward) 5'-CCGGAATCAGAAACAAAAGAATGT-3' and (reverse) 5'-CTTGGGGAGCACAATGAGCA-3'; signal transducer and activator of transcription 3 (*Stat3*) (forward) 5'-AGTTCCTGGCACCTTGGATT-3' and (reverse) 5'-CGATCCGGGCAATTTCCATT-3'. Reactions were performed using Fast SYBR Green Mastermix (Life Technologies) on a 7900HT Fast Real-Time PCR System (Applied Biosystems). PCR conditions were programmed as follows: 95°C for 20 s, followed by 40 cycles of denaturing at 95°C for 1 s, annealing and extension at 58°C for 20 s, followed by a standard dissociation curve. A dilution series of template DNA served as an internal standard for quantification (36). Data represent the transcript level of the gene of interest (as expressed as a copy number) normalized to the copy number of the housekeeping gene *18s*.

Immunoblot analysis

Protein was harvested from prostate lobes using a handheld pestle (Thermo Fisher), and radioimmunoprecipitation assay protein lysis buffer (Thermo Fisher) supplemented with protease inhibitor cocktail (Thermo Fisher) and processed as previously described (37). Equal amounts of protein were separated on NuPage Bis-Tris SDS-PAGE gels (Thermo Fisher) and blotted to a polyvinylidene difluoride or nitrocellulose membrane (Bio-Rad, Hercules, CA) in accordance with the manufacturer's protocol (Thermo Fisher). Membranes were blocked overnight with 5% powdered milk in PBS with Tween 20 at 4°C and then probed for the indicated proteins following standard protocols using anti-p16 (10,883; Proteintech) and β -actin (A5441) (Sigma-Aldrich) antibodies at 1:200 and 1:10,000 dilutions, respectively. Goat anti-rabbit (1:1000 dilution), or goat anti-mouse (1:50,000 dilution) secondary antibodies were also used (Santa Cruz Biotechnology) using standard conditions. Membranes were incubated in SuperSignal West Femto Reagent (Thermo Fisher) and developed on the ChemiDoc MP imaging system for visualization (Bio-Rad). Densitometric analyses were performed on the native membrane image using Image Lab 4.0 software (Bio-Rad). The relative densitometric value of each replicate for p16 was normalized to the corresponding relative level of β -actin and expressed relative to the mean amount found in mice fed a control diet.

Statistical analysis

All data were graphed in GraphPad Prism 5 software (La Jolla, CA) with bars indicating the mean \pm SEM. To determine if there were statistically significant differences between groups for continuous variables, both 2-factor ANOVA and unpaired *t* tests were performed. For categorical variables, we used either Fisher's exact or chi-square tests to compare groups. Cochran-Armitage tests were conducted for trend analysis. Bonferroni corrections (also known as Bonferroni post-tests) were used to account for multiple comparisons. A statistically significant difference between groups was noted for *P* values <0.05.

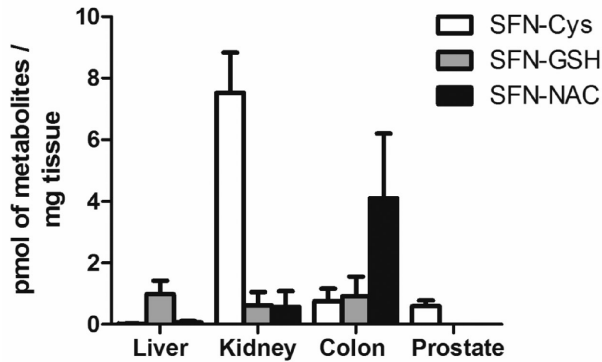


FIGURE 1 SFN metabolites were detectable in mice fed a diet rich in broccoli sprouts. SFN-Cys, SFN-GSH, and SFN-NAC were detected in the indicated organs of mice on 15% broccoli sprout diet at 12 wk of age ($n = 3-6$). SFN metabolites were not detected in control mice. SFN, sulforaphane; SFN-Cys, SFN-cysteine; SFN-GSH, SFN-glutathione; SFN-NAC, SFN-*N*-acetylcysteine.

Results

Broccoli sprout consumption slowed prostate cancer formation and decreased cancer severity

Mice fed the 15% broccoli sprout diet had detectable amounts of SFN metabolites in liver, kidney, colon, and prostate tissues (Figure 1). SFN-cysteine was the most abundant metabolite in the kidney and prostate, whereas SFN-glutathione was highest in the liver. SFN-NAC was the most abundant SFN metabolite in the colon. The parent compound and SFN-cysteinylglycine were not detected in any samples tested. The mean total SFN metabolites were 1.1, 8.7, 5.8, and 0.6 pmol SFN/mg tissue for the liver, kidney, colon, and prostate, respectively. SFN metabolites were not detected in control mice (data not shown).

In the TRAMP model, the SV40 transgene expression is turned on at sexual maturity between 8 and 10 wk of age. Following this, mouse prostatic intraepithelial neoplasia (mPIN) lesions are seen at 12 wk of age. By 28 wk, adenocarcinomas and metastasis can occur (31–33). As expected, both the urogenital tract and prostate weights increased with age in control mice (Figure 2A, B). At the 12-wk time point, urogenital tract weight and prostate weight in mice on the high broccoli sprout diet were 2.8- and 2.3-fold lower, respectively, than in mice on the control diet (Figure 2A, B). At 28 wk of age the effect of broccoli sprout diet was not as apparent on urogenital tract and prostate weights, and there was no significant differences between the mice on control and broccoli sprout diet (Figure 2A, B).

Prostate cancer incidence and severity was significantly reduced in the broccoli sprout groups at both the 12- and 28-wk time points (Figure 2C–E). At 12 wk of age all control mice developed at least early neoplastic lesions (mPIN), whereas 7 out of 20 of the broccoli sprout-fed mice had normal prostates (Figure 2C, D). Furthermore, only 1 broccoli sprout-fed mouse developed an adenocarcinoma, whereas 10 out of 18 control mice had adenocarcinomas at 12 wk of age (Figure 2C, D). By 28 wk of age, 16 out of 18 control mice had an adenocarcinoma, whereas only 7 out of 19 broccoli sprout-fed mice had cancer that had advanced to this state (Figure 2C, E). It is also worth noting that at the point at which they were euthanized, 2 of the broccoli sprout-fed mice

had developed no prostate lesions (Figure 2C). Importantly, consumption of a diet high in broccoli sprouts significantly reduced the incidence of invasive prostate cancer by 11- and 2.4-fold, at the 12- and 28-wk time points, respectively (Figure 2F).

Broccoli sprout consumption decreased HDAC3 expression in prostate epithelium

To determine if HDAC protein expression was altered in prostate epithelium, we performed immunohistochemistry using antibodies against HDAC3 and HDAC6. We focused on these HDACs because HDAC3 is highly expressed in prostate cancer and HDAC6 regulates androgen receptor signaling, and both HDACs are decreased by SFN treatment in *in vitro* models of cancer (22, 23, 28, 38–40). A significant decline in HDAC3 protein expression was detected in the ventral and anterior lobes of the prostate of mice fed broccoli sprout diet (Figure 3A, B). The broccoli sprout-induced decline in HDAC3 protein was more apparent at the 12-wk time point (Figure 3B). We did not detect a significant change in HDAC6 protein abundance in the prostates of broccoli sprout-fed mice at 12 or 28 wk of age (Figure 4A, B). It is worth noting that HDAC6 protein appeared lower with broccoli sprouts at the 28-wk time point in the ventral lobe of the prostate, and a *t* test confirmed a trend for decreased HDAC6 with broccoli sprouts in this lobe (Figure 4B, *t* test, $P = 0.056$).

Broccoli sprout-induced changes in histone modifications in TRAMP mouse prostates

HDACs regulate gene expression by removing acetylation marks from histones (41). Since H3K18 and H3K9 acetylation have been shown to be regulated by HDAC3, we tested if broccoli sprout-mediated decrease in HDAC3 expression resulted in alterations in H3K18 and H3K9 acetylation levels in the prostate (42). Surprisingly, broccoli sprout diet induced a significant 2-fold decline in H3K18 acetylation levels in all prostate lobes at the 28-wk time point (Figure 5A, B). There was no significant change in H3K18ac at 12 wk when HDAC3 protein was significantly decreased, and thus no correlation between HDAC3 and H3K18 acetylation was detected (Figures 3 and 5B). We did not detect a significant change in acetylation of H3K9 residues in the prostate of mice fed broccoli sprouts, but we did find a significant age effect in the anterior lobe of the prostate (Supplemental Figure 1). Since we did not find the expected changes in acetylation of histones, we next examined if consumption of broccoli sprouts altered H3K9me3, which has been previously reported to decrease *in vitro* following SFN treatment in PC-3 prostate cancer cells and is altered with HDAC3 deletion (26, 43). More specifically, because the anterior lobe of the prostate exhibited a marked loss of HDAC3, we examined the area, intensity, and number of H3K9me3 foci, and noted H3K9me3 punctate staining in the nucleus. A significant decline in H3K9me3 also occurred with age, but there was no apparent effect of diet (Supplemental Figure 2A). We next focused our examination of H3K9me3 levels in the ventral lobe at the 12-wk time point, because this was when HDAC3 was significantly downregulated. A significant 13% decrease in the mean area/foci for H3K9me3 staining was found with broccoli sprout consumption in the ventral lobe (Supplemental Figure 2B).

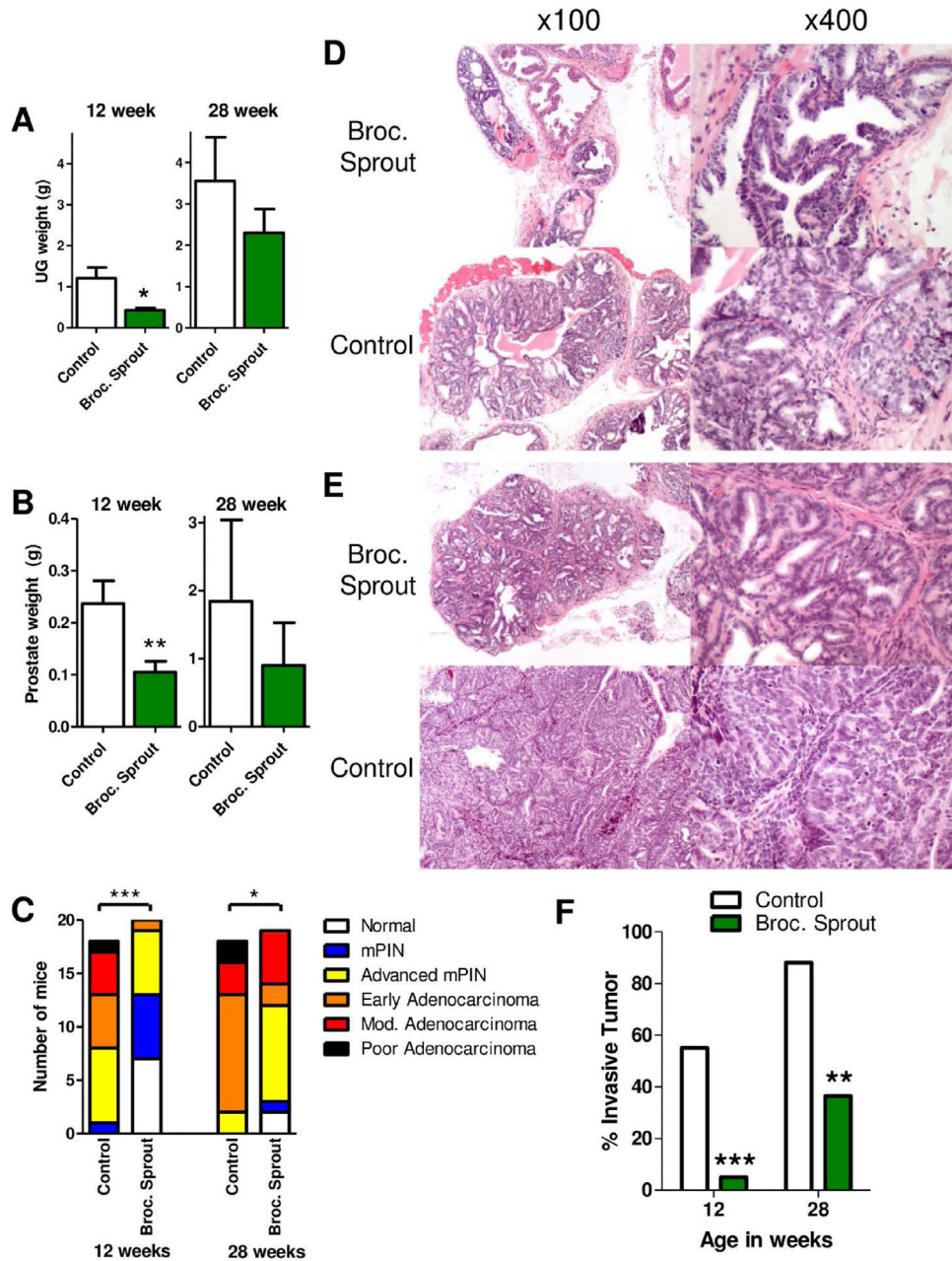


FIGURE 2 Broccoli sprout consumption suppressed prostate cancer development. TRAMP mice were fed the indicated control or 15% broccoli sprout diet and evaluated for (A) UG tract weight, (B) prostate weight, and (C–F) the presence and severity of lesions associated with prostate cancer, at 12 and 28 wk of age ($n = 17–20$). (A, B) Statistical significance was calculated using a t test where * and ** indicate significant differences between the groups at $P < 0.05$ and $P < 0.01$, respectively. (C) Colors indicate the number and distribution of mice with the indicated tumor grade level by dietary intake and age ($n = 18–20$). Cochran-Armitage trend test was used to evaluate differences in tumor grade level between control and broccoli sprout–fed groups where at 12 wk *** indicates $P < 0.0001$ and 28 wk * indicates $P = 0.019$. (D, E) H&E-stained sections of prostate tissue at (D) 12 and (E) 28 wk of age; left column 100 \times ; right column 200 \times . (D) mPIN is evident in the anterior prostate lobe of both control and broccoli sprout–fed mice. However, cribriform mPIN is diffuse and pronounced in control mice in contrast to the multifocal distribution of early mPIN in broccoli sprout–fed mice. Note, mitotic figures are more frequent in the latter, but cellular and nuclear atypia more prominent in control prostates. (E) Well-differentiated, cribriform to tubular adenocarcinoma in the prostate of a broccoli sprout–fed mouse is smaller and has low cellular atypia compared to moderately differentiated adenocarcinoma with numerous mitotic figures and noticeable cellular atypia in a control prostate. (F) Bars indicate the percentage of mice with an invasive tumor at the indicated age and diet. Mice with normal prostates, and mice with mPIN and advanced mPIN, were considered noninvasive. Early, moderate, and poorly differentiated adenocarcinomas were grouped as invasive tumors. Statistical significance was calculated using a Fisher exact test where ** and *** indicate significant differences between the groups at $P < 0.01$ and $P < 0.001$, respectively. Broc., broccoli; H&E, hematoxylin and eosin; Mod., moderate; mPIN, mouse prostatic intraepithelial neoplasia; TRAMP, transgenic adenocarcinoma of the mouse prostate; UG, urogenital.

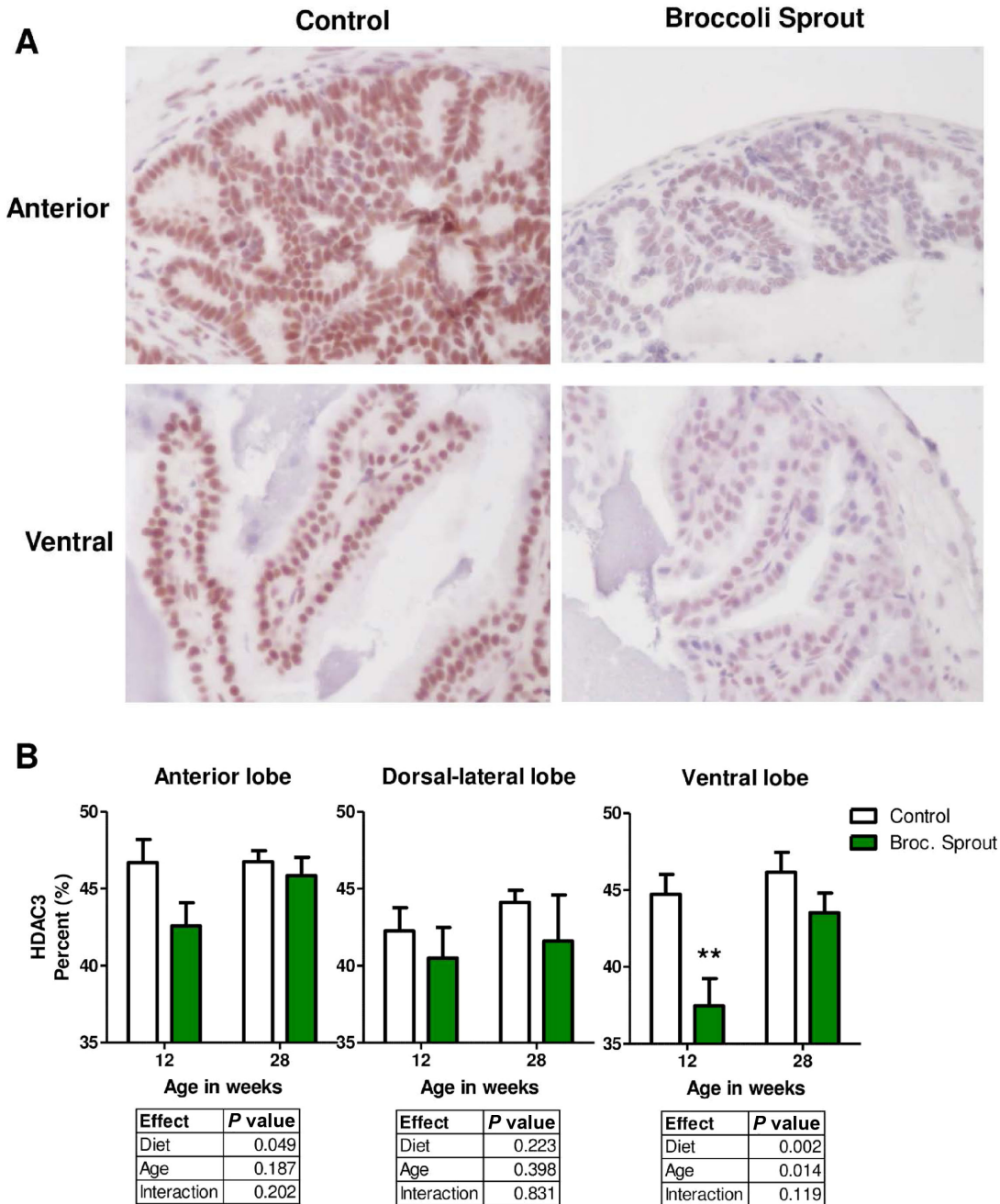


FIGURE 3 Broccoli sprouts decreased HDAC3 protein in prostate epithelial cells. (A, B) HDAC3 was detected in the prostate lobes of TRAMP mice fed control or 15% broccoli sprout diet using immunohistochemistry. Chromagen Nova Red; counterstain hematoxylin. (A) Representative images of HDAC3 staining in anterior and ventral prostate lobes at 12 wk of age taken at 400× magnification. (B) HDAC3 staining intensity quantification, in which staining is expressed as a percentage of all possible color. Significant differences between samples were calculated using 2-factor ANOVAs with results detailed in individual tables for each prostate lobe ($n = 9-15$, except for dorsal-lateral with broccoli sprout where $n = 4-7$). Bonferroni post-tests were used to determine differences between control and broccoli sprout groups where ** indicates a significant difference between the groups at $P < 0.01$. Broc., broccoli; HDAC3, histone deacetylase 3; TRAMP, transgenic adenocarcinoma of the mouse prostate.

Effect of broccoli sprout diet on the expression on HDAC3 target genes

To gain further insights into how decreases in HDAC3 by broccoli sprouts could slow prostate cancer progression, we evaluated the

expression of several genes that are known to be regulated by HDAC3. We examined the mRNA expression of *p16* [also known as cyclin-dependent kinase inhibitor 2A (*CDKN2A*)], *STAT3*, retinoblastoma binding protein 8, endonuclease (*RBBP8* also known as *CTIP*), and

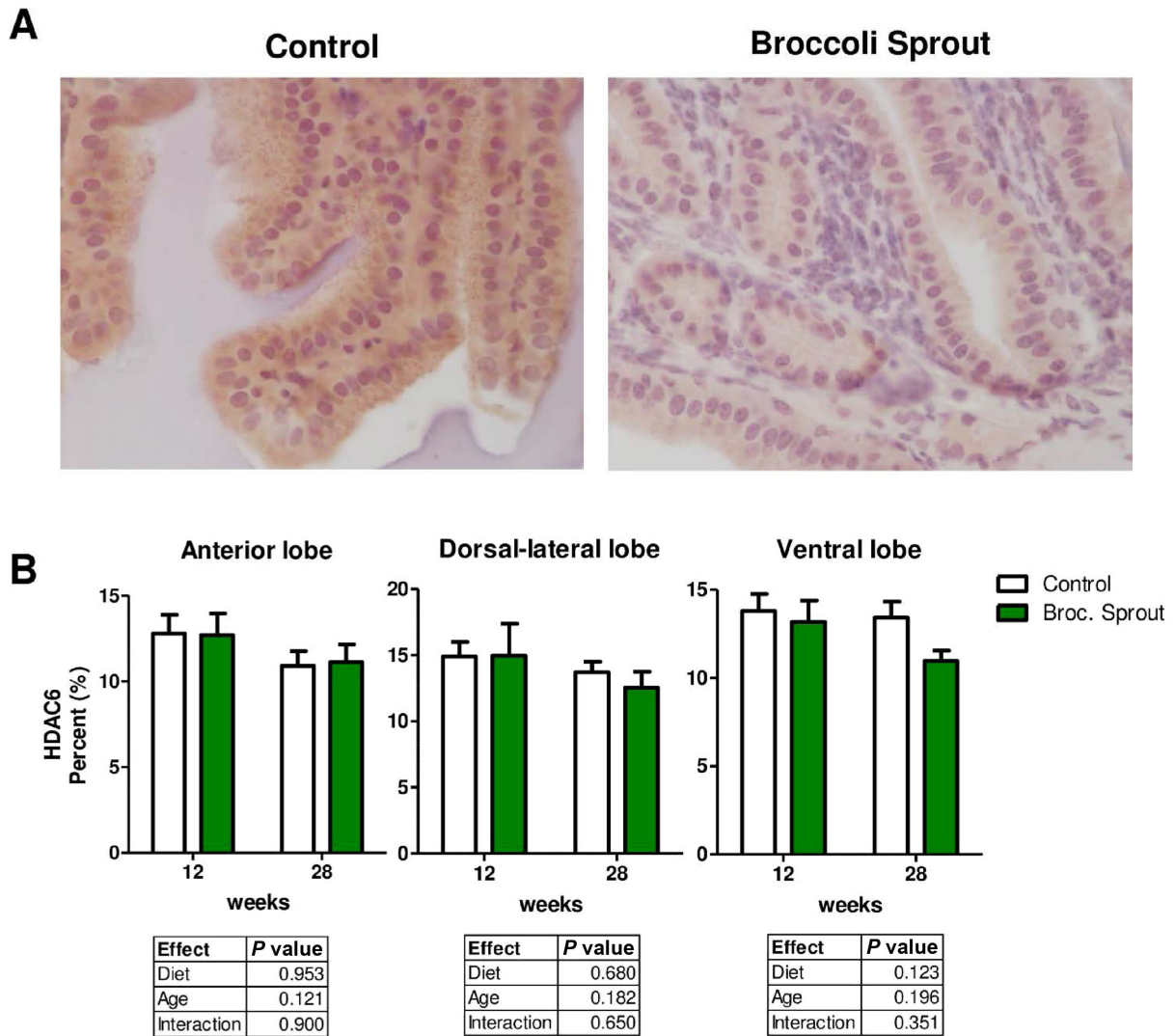


FIGURE 4 Trend of decreased HDAC6 protein in the ventral prostate lobe with broccoli sprouts. (A, B) HDAC6 was detected using immunohistochemistry in the prostate lobes of TRAMP mice fed control, or 15% broccoli sprout diet. Chromagen Nova Red; counterstain hematoxylin. (A) Representative images of HDAC6 staining in ventral prostate lobe at 28 wk of age taken at 400 \times magnification. (B) HDAC6 staining intensity quantification in which staining is expressed as a percentage of all possible color. Significant differences between samples were calculated using 2-factor ANOVAs with results detailed in individual tables for each prostate lobe ($n = 6-16$). Broc., broccoli; HDAC6, histone deacetylase 6; TRAMP, transgenic adenocarcinoma of the mouse prostate.

SERPINB5 (38, 44, 45). This work was done in TRAMP prostates of 12-wk-old mice when HDAC3 was decreased with broccoli sprouts. As a positive control, we examined the expression of a known target of SFN, the NAD(P)H quinone dehydrogenase 1 gene (*NQO1*), and show that its mRNA level was significantly upregulated with broccoli sprout consumption in the dorsolateral lobe of the prostate [Figure 6A, and (46)]. We found significant differences in the expression of mRNA in all 5 genes when compared among the different prostate lobes (Figure 6 and Supplemental Figure 3). No significant effect of broccoli sprout consumption on the mRNA levels of *RBBP8* and *SERPINB5* was detected, although there was a trend for increased expression of *STAT3* with broccoli sprout consumption (Supplemental Figure 3A-C). Unexpectedly, the tumor suppressor gene *p16* was significantly decreased at

the mRNA level with broccoli sprout consumption in all prostate lobes (Figure 6B). This coincided with the time point when HDAC3 was decreased. Western blotting revealed no change in the amount of p16 at the protein level (Figure 6C). We also examined p21 protein expression, but it was not detectable in the prostate lobes (data not shown).

Discussion

Given the high incidence and mortality associated with prostate cancer worldwide, reducing prostate cancer incidence and slowing progression is of great importance. The WHO has identified that between 30% and 50% of the current global cancer burden could be prevented, and

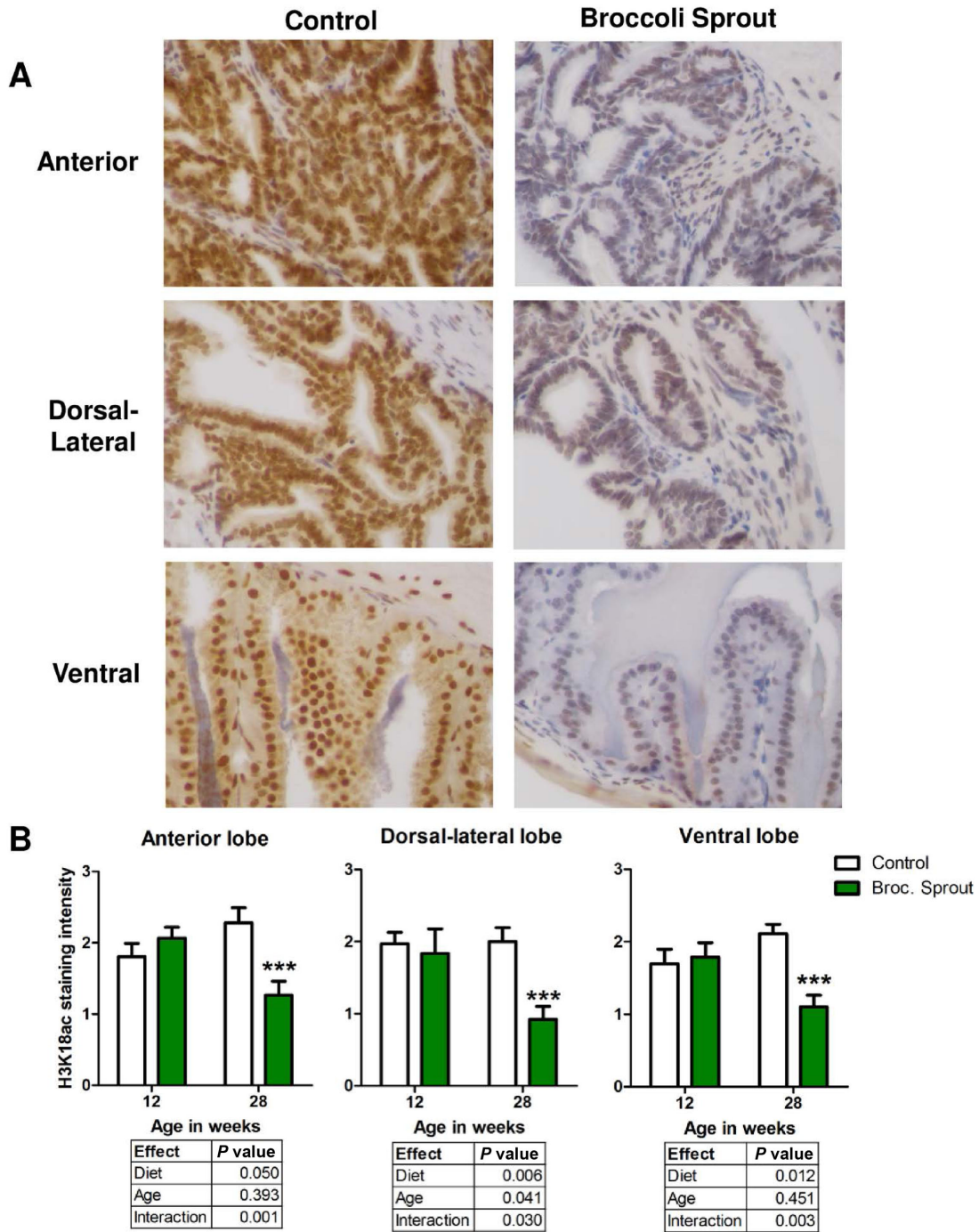


FIGURE 5 Broccoli sprouts decreased H3K18ac in prostate epithelial cells. (A, B) H3K18ac was detected using immunohistochemistry in the prostate lobes of TRAMP mice fed control or 15% broccoli sprout diet. Chromagen Nova Red; counterstain hematoxylin. (A) Representative images of H3K18ac staining in indicated prostate lobes at 28 wk of age taken at 400× magnification. (B) H3K18 acetylation was quantified on a scale from 0 to 3. Significant differences between samples were calculated using 2-factor ANOVAs with results detailed in individual tables for each prostate lobe (n = 9–18). Bonferroni post-tests were used to determine differences between mice fed a control and broccoli sprout diet where *** indicates a significant difference between the groups at P < 0.001. Broc., broccoli; H3K18ac, acetyl-histone H3 lysine 18; TRAMP, transgenic adenocarcinoma of the mouse prostate.

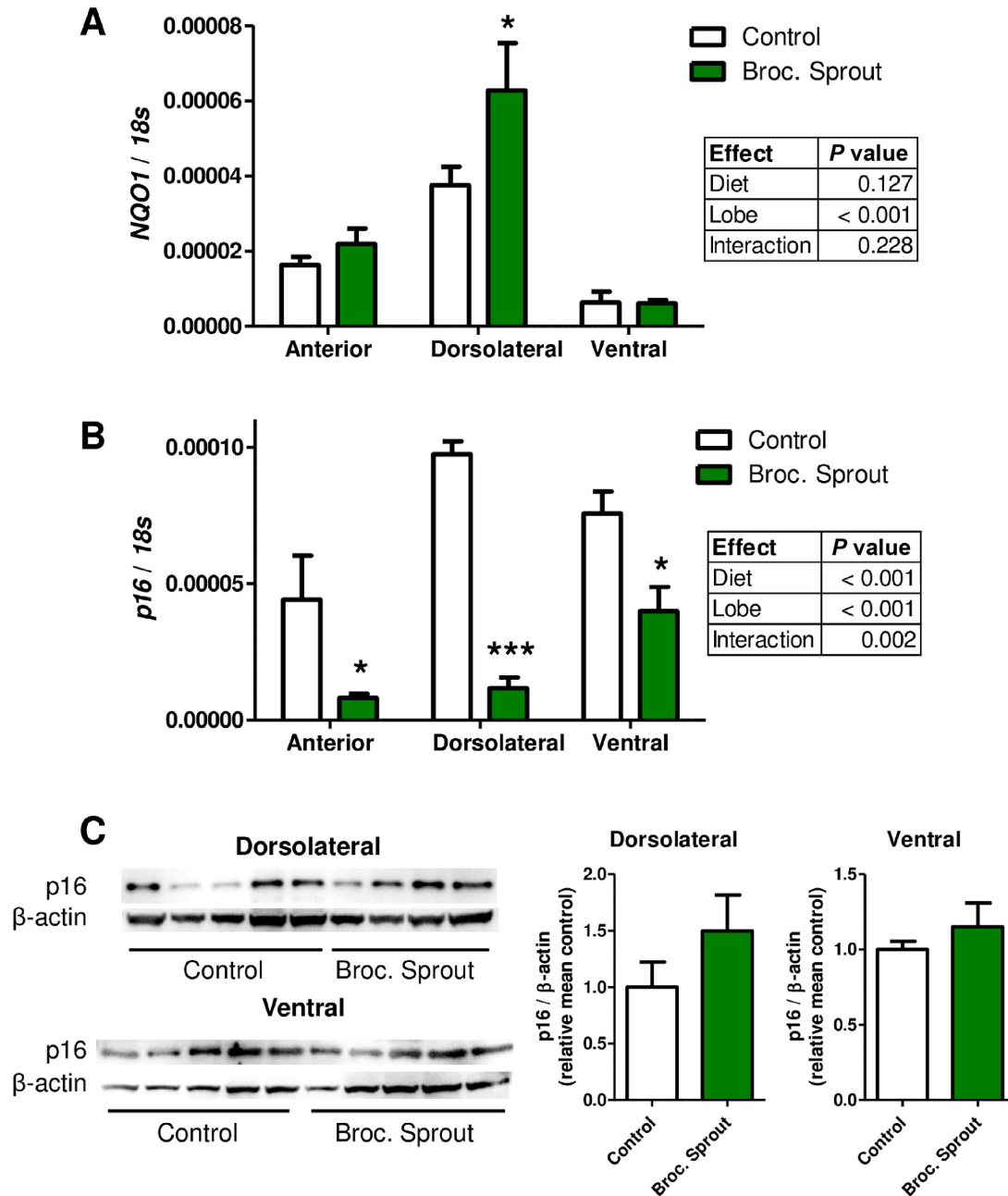


FIGURE 6 Broccoli sprouts decreased *p16* mRNA levels but did not significantly alter *p16* protein abundance. Bars represent mean (A) mRNA levels of *NQO1*, (B) mRNA levels of *p16*, or (C) *p16* protein levels in prostate lobes of mice feed a control diet (white bars) or 15% broccoli sprout diet (green bars). Tissue was collected at 12 wk of age. (A, B) Significant differences between groups were calculated using 2-factor ANOVAs with results detailed in individual tables for each gene. Bonferroni post-tests were used to determine differences between control or broccoli sprout groups where * and *** indicate significant differences between the groups at $P < 0.05$ and $P < 0.001$, respectively ($n = 4-7$). (C) Images are representative Western blots of mouse prostate tissue analyzed for *p16* protein abundance, with corresponding densitometry results where no significant differences between control and broccoli sprout groups were detected (t test, $P > 0.05$). Broc., broccoli; *NQO1*, *NAD(P)H:quinone oxidoreductase 1*.

indicate that an unhealthy diet and low fruit and vegetable intake are key modifying risk factors for cancer development (47). Here we show in a preclinical model that consumption of a diet high in broccoli sprouts results in detectable amounts of SFN metabolites in the prostate and reduced prostate cancer incidence and severity. We show for the first time, to our knowledge, that a diet high in cruciferous vegetables can decrease HDAC expression, primarily HDAC3, in the prostate epithelial cells at a time when prostate cancer is developing. We also show that a broccoli sprout diet causes significant changes in some epigenetic marks, with broccoli-induced declines in the acetylation of histone H3 lysine 18 being the most notable.

The TRAMP model of prostate cancer was utilized because the tumors occur in the prostate epithelium and the tumor tissue histopathology closely mimics human disease. Additional advantages include that the tumors arise spontaneously and appear in ~100% of mice (31–33). The cancer is driven by the oncoprotein SV40 T antigen which binds to p53 and retinoblastoma proteins, disrupting their tumor suppressor function and the normal signaling circuitry that controls cell cycle (48). Our data are in agreement with several studies in TRAMP mice wherein a diet high in broccoli sprouts, or treatment with SFN, suppressed prostate cancer development and/or metastasis (8, 14, 15, 49). Overall, this literature suggests that broccoli sprouts (and/or SFN) are acting through multiple mechanisms to decrease prostate cancer development, including inhibition of cell cycle, inhibition of the chemokine receptor CXCR4, and increased apoptosis via mechanisms such as inhibition of the Akt signaling pathway (8, 14, 49). In contrast to these studies, Liu et al. (16) did not find a significant effect of broccoli sprout diet on prostate cancer, although they used a lower amount of broccoli sprouts (10% broccoli sprout powder), and started the mice on the diet at a later age than in our study.

Our finding of a broccoli-induced decrease in HDAC3 protein is significant because HDAC3 is highly expressed in carcinomas of prostate cancer patients, and upregulation of class-I HDACs are thought to be an early event in prostate carcinogenesis (40). Our results are consistent with previous work showing inhibition of HDAC3 with broccoli-related supplements in preclinical models of colon and skin cancer, and in clinical studies looking at human breast tissue and blood cells (27–29). Together, these studies show that HDAC3 is suppressed following broccoli sprout consumption across multiple tissue types and species. The mechanism by which SFN induces HDAC3 degradation has been previously described in colon cancer cells and is likely similar in prostate tissue, involving disruption of corepressor interactions and increased nuclear-cytoplasmic trafficking (23). We did not see a significant decrease of HDAC3 when the prostate cancer was more advanced. It is not clear why this effect was lost, and future work will have to explore this phenomenon. One issue that may contribute to the loss of some of the expected effects is the adaptation of the organism and/or cancer to a high-broccoli sprout diet that was consumed over the majority of the mice's life. HDAC6 has been observed to be inhibited and/or decreased by SFN in cultured prostate cancer cells (22, 39). We saw only a trend of decreasing HDAC6 protein with broccoli sprout consumption. It will be interesting for future work to determine if HDAC3 or HDAC6 expression is suppressed in prostate biopsies of men who have consumed broccoli sprout or related supplements.

We encountered limitations with the TRAMP model when we found that a diet high in broccoli sprouts significantly decreased H3K18ac

and p16 mRNA levels. Inhibition of HDAC3 is generally thought to increase histone acetylation, and increased expression of p16 has previously been observed in human peripheral blood mononuclear cells following consumption of broccoli sprout extracts, and in colon tumors of wild-type mice treated with SFN (28). We cannot rule out effects of the dietary treatments on histone acetyltransferases, which coordinate with HDACs to regulate overall histone acetylation status. Previous changes in epigenetic targets reported with SFN may be different than what is observed with a whole-food approach tested here, as the food has added components that could cause differences in downstream molecular mechanisms. It is important to note, however, that in the TRAMP model the large T antigen is known to upregulate p16 expression and promote global H3K18 hypoacetylation through interactions with the histone acetyltransferases p300 and CBP, and this is likely effecting the epigenetic targets studied here (50–53). Our study cannot directly confirm large T antigen effects on p16 or H3K18ac because we did not follow these endpoints over a continuum of prostate cancer development. Nevertheless, it is encouraging that the broccoli-induced alterations in p16 mRNA and H3K18ac levels we observed were correcting for changes that are thought to contribute to cancer promotion in this model (52, 53). The changes in cell signaling induced by the large T-antigen are also the likely mechanism for why no changes in p16 protein abundance was found (50, 51). Interestingly, p16 overexpression has been found in human benign tumors, high-grade malignancies, and in a specific mouse model of colon cancer, where SFN treatment decreased p16 protein levels when the mice were heterozygous for the gene *Nrf2* (28, 54, 55).

Broccoli sprout consumption also decreased the area of H3K9 trimethylation in the ventral prostate lobe at the same time as HDAC3 decreased. This decline in H3K9 trimethylation is consistent with a previous report in our laboratory showing that SFN decreased global H3K9me3 by modifying the histone methyltransferase SUV39H1 (26). Taken together, the data from this study support the hypothesis that broccoli-induced alteration of the epigenetic landscape is likely one important mechanism by which a diet high in broccoli sprouts contributes to prostate cancer chemoprevention. The study also highlights that the cellular context in which a chemopreventive treatment is given is critical in determining the expected molecular endpoints, and points to the need to conduct studies using human clinical samples when possible.

Acknowledgments

We thank Kay Fischer and her team at the Oregon Veterinary Diagnostics Laboratory and Drs Kelli Lytle, David Yu, Rong Wang at Oregon State University and Dr George Thomas at Oregon Health & Science University for technical assistance and helpful conversations. We also thank Dr Praveen Rajendran at Texas A&M Health Science Center for helpful conversation on HDAC3 target genes. We are grateful to Amanda Hilman and Justin Brown at OHSU for their technical work with animal breeding, genotyping, and husbandry.

The authors' responsibilities were as follows—EH, RHD, DEW, JS, and PT: designed the research; PT: provided essential material; LMB, CVL, GWW, JDC, STG, CPW, and PT: conducted the research; CVL, LMB, GWW, JDC, and ZZ: analyzed the data; LMB: wrote the article; EH: had primary responsibility for the final content; and all authors: read and approved the final manuscript.

References

- International Agency for Research on Cancer, Cancer Fact Sheet: Prostate Cancer 2012, GLOBOCAN 2012, World Health Organization, date of acquisition: 12 October 2017; electronic data sheet available from: <http://globocan.iarc.fr/old/FactSheets/cancers/prostate-new.asp>
- Siegel RL, Miller KD, Jemal A. Cancer statistics, 2017. *CA Cancer J Clin* 2017;67:7–30.
- Brawn PN, Speights VO, Contin JU, Bayardo RJ, Kuhl DL. Atypical hyperplasia in prostates of 20 to 40 year old men. *J Clin Pathol* 1989;42:383–6.
- Sakr WA, Haas GP, Cassin BF, Pontes JE, Crissman JD. The frequency of carcinoma and intraepithelial neoplasia of the prostate in young male patients. *J Urol* 1993;150(2 Pt 1):379–85.
- Haas GP, Delongchamps N, Brawley OW, Wang CY, de la Roza G. The worldwide epidemiology of prostate cancer: perspectives from autopsy studies. *Can J Urol* 2008;15:3866–71.
- Liu B, Mao Q, Cao M, Xie L. Cruciferous vegetables intake and risk of prostate cancer: a meta-analysis. *Int J Urol* 2012;19:134–41.
- Higdon JV, Delage B, Williams DE, Dashwood RH. Cruciferous vegetables and human cancer risk: epidemiologic evidence and mechanistic basis. *Pharmacol Res* 2007;55:224–36.
- Singh SV, Warin R, Xiao D, Powolny AA, Stan SD, Arlotti JA, Zeng Y, Hahm ER, Marynowski SW, Bommareddy A, et al. Sulforaphane inhibits prostate carcinogenesis and pulmonary metastasis in TRAMP mice in association with increased cytotoxicity of natural killer cells. *Cancer Res* 2009;69:2117–25.
- Keum YS, Khor TO, Lin W, Shen G, Kwon KH, Barve A, Li W, Kong AN. Pharmacokinetics and pharmacodynamics of broccoli sprouts on the suppression of prostate cancer in transgenic adenocarcinoma of mouse prostate (TRAMP) mice: implication of induction of Nrf2, HO-1 and apoptosis and the suppression of Akt-dependent kinase pathway. *Pharm Res* 2009;26:2324–31.
- Agyeman AS, Chaerkady R, Shaw PG, Davidson NE, Visvanathan K, Pandey A, Kensler TW. Transcriptomic and proteomic profiling of KEAP1 disrupted and sulforaphane-treated human breast epithelial cells reveals common expression profiles. *Breast Cancer Res Treat* 2012;132:175–87.
- Thimmulappa RK, Mai KH, Srisuma S, Kensler TW, Yamamoto M, Biswal S. Identification of Nrf2-regulated genes induced by the chemopreventive agent sulforaphane by oligonucleotide microarray. *Cancer Res* 2002;62:5196–203.
- Hu R, Xu C, Shen G, Jain MR, Khor TO, Gopalkrishnan A, Lin W, Reddy B, Chan JY, Kong AN. Gene expression profiles induced by cancer chemopreventive isothiocyanate sulforaphane in the liver of C57BL/6J mice and C57BL/6J/Nrf2 (-/-) mice. *Cancer Lett* 2006;243:170–92.
- Zhang C, Su ZY, Khor TO, Shu L, Kong AN. Sulforaphane enhances Nrf2 expression in prostate cancer TRAMP C1 cells through epigenetic regulation. *Biochem Pharmacol* 2013;85:1398–404.
- Sakao K, Vyas AR, Chinni SR, Amjad AI, Parikh R, Singh SV. CXCR4 is a novel target of cancer chemopreventive isothiocyanates in prostate cancer cells. *Cancer Prev Res* 2015;8:365–74.
- Vyas AR, Hahm ER, Arlotti JA, Watkins S, Stolz DB, Desai D, Amin S, Singh SV. Chemoprevention of prostate cancer by d,l-sulforaphane is augmented by pharmacological inhibition of autophagy. *Cancer Res* 2013;73:5985–95.
- Liu AG, Juvik JA, Jeffery EH, Berman-Booty LD, Clinton SK, Erdman JW Jr. Enhancement of broccoli indole glucosinolates by methyl jasmonate treatment and effects on prostate carcinogenesis. *J Med Food* 2014;17:1177–82.
- Hanahan D, Weinberg RA. Hallmarks of cancer: the next generation. *Cell* 2011;144:646–74.
- Wang L, Zou X, Berger AD, Twiss C, Peng Y, Li Y, Chiu J, Guo H, Satagopan J, Wilton A, et al. Increased expression of histone deacetylases (HDACs) and inhibition of prostate cancer growth and invasion by HDAC inhibitor SAHA. *Am J Transl Res* 2009;1:62–71.
- Ashktorab H, Belgrave K, Hosseinkhah F, Brim H, Nouraei M, Takkikto M, Hewitt S, Lee EL, Dashwood RH, Smoot D. Global histone H4 acetylation and HDAC2 expression in colon adenoma and carcinoma. *Dig Dis Sci* 2009;54:2109–17.
- Bolden JE, Peart MJ, Johnstone RW. Anticancer activities of histone deacetylase inhibitors. *Nat Rev Drug Discov* 2006;5:769–84.
- Meeran SM, Patel SN, Tollefsbol TO. Sulforaphane causes epigenetic repression of hTERT expression in human breast cancer cell lines. *PLoS One* 2010;5:e11457.
- Clarke JD, Hsu A, Yu Z, Dashwood RH, Ho E. Differential effects of sulforaphane on histone deacetylases, cell cycle arrest and apoptosis in normal prostate cells versus hyperplastic and cancerous prostate cells. *Mol Nutr Food Res* 2011;55:999–1009.
- Rajendran P, Delage B, Dashwood WM, Yu TW, Wuth B, Williams DE, Ho E, Dashwood RH. Histone deacetylase turnover and recovery in sulforaphane-treated colon cancer cells: competing actions of 14-3-3 and Pin1 in HDAC3/SMRT corepressor complex dissociation/reassembly. *Mol Cancer* 2011;10:68.
- Hsu A, Wong CP, Yu Z, Williams DE, Dashwood RH, Ho E. Promoter de-methylation of cyclin D2 by sulforaphane in prostate cancer cells. *Clin Epigenetics* 2011;3:3.
- Wong CP, Hsu A, Buchanan A, Palomera-Sanchez Z, Beaver LM, Houseman EA, Williams DE, Dashwood RH, Ho E. Effects of sulforaphane and 3,3'-diindolylmethane on genome-wide promoter methylation in normal prostate epithelial cells and prostate cancer cells. *PLoS One* 2014;9:e86787.
- Watson GW, Wickramasekara S, Palomera-Sanchez Z, Black C, Maier CS, Williams DE, Dashwood RH, Ho E. SUV39H1/H3K9me3 attenuates sulforaphane-induced apoptotic signaling in PC3 prostate cancer cells. *Oncogenesis* 2014;3:e131.
- Su ZY, Zhang C, Lee JH, Shu L, Wu TY, Khor TO, Conney AH, Lu YP, Kong AN. Requirement and epigenetics reprogramming of Nrf2 in suppression of tumor promoter TPA-induced mouse skin cell transformation by sulforaphane. *Cancer Prev Res* 2014;7:319–29.
- Rajendran P, Dashwood WM, Li L, Kang Y, Kim E, Johnson G, Fischer KA, Lohr CV, Williams DE, Ho E, et al. Nrf2 status affects tumor growth, HDAC3 gene promoter associations, and the response to sulforaphane in the colon. *Clin Epigenetics* 2015;7:102.
- Atwell LL, Zhang Z, Mori M, Farris P, Vetto JT, Naik AM, Oh KY, Thuillier P, Ho E, Shannon J. Sulforaphane bioavailability and chemopreventive activity in women scheduled for breast biopsy. *Cancer Prev Res* 2015;8:1184–91.
- Myzaks MC, Tong P, Dashwood WM, Dashwood RH, Ho E. Sulforaphane retards the growth of human PC-3 xenografts and inhibits HDAC activity in human subjects. *Exp Biol Med* 2007;232:227–34.
- Greenberg NM, DeMayo F, Finegold MJ, Medina D, Tilley WD, Aspinall JO, Cunha GR, Donjacour AA, Matusik RJ, Rosen JM. Prostate cancer in a transgenic mouse. *Proc Natl Acad Sci U S A* 1995;92:3439–43.
- Greenberg NM. Transgenic models for prostate cancer research. *Urol Oncol* 1996;2:119–22.
- Gingrich JR, Greenberg NM. A transgenic mouse prostate cancer model. *Toxicol Pathol* 1996;24(4):502–4.
- Parisotto M, Metzger D. Genetically engineered mouse models of prostate cancer. *Mol Oncol* 2013;7:190–205.
- Clarke JD, Hsu A, Williams DE, Dashwood RH, Stevens JF, Yamamoto M, Ho E. Metabolism and tissue distribution of sulforaphane in Nrf2 knockout and wild-type mice. *Pharm Res* 2011;28:3171–9. Epub 2011/06/18.
- Wong CP, Magnusson KR, Ho E. Increased inflammatory response in aged mice is associated with age-related zinc deficiency and zinc transporter dysregulation. *J Nutr Biochem* 2013;24:353–9.
- Watson GW, Wickramasekara S, Fang Y, Maier CS, Williams DE, Dashwood RH, Perez VI, Ho E. HDAC6 activity is not required for basal autophagic flux in metastatic prostate cancer cells. *Exp Biol Med (Maywood)* 2016;241:1177–85.
- Rajendran P, Kidane AI, Yu TW, Dashwood WM, Bisson WH, Lohr CV, Ho E, Williams DE, Dashwood RH. HDAC turnover, CtIP acetylation and

- dysregulated DNA damage signaling in colon cancer cells treated with sulforaphane and related dietary isothiocyanates. *Epigenetics* 2013;8:612–23.
39. Gibbs A, Schwartzman J, Deng V, Alumkal J. Sulforaphane destabilizes the androgen receptor in prostate cancer cells by inactivating histone deacetylase 6. *Proc Natl Acad Sci U S A* 2009;106:16663–8.
 40. Weichert W, Roske A, Gekeler V, Beckers T, Stephan C, Jung K, Fritzsche FR, Niesporek S, Denkert C, Dietel M, et al. Histone deacetylases 1, 2 and 3 are highly expressed in prostate cancer and HDAC2 expression is associated with shorter PSA relapse time after radical prostatectomy. *Br J Cancer* 2008;98:604–10.
 41. Seto E, Yoshida M. Erasers of histone acetylation: the histone deacetylase enzymes. *Cold Spring Harb Perspect Biol* 2014;6:a018713.
 42. Zhang X, Wharton W, Yuan Z, Tsai SC, Olashaw N, Seto E. Activation of the growth-differentiation factor 11 gene by the histone deacetylase (HDAC) inhibitor trichostatin A and repression by HDAC3. *Mol Cell Biol* 2004;24:5106–18.
 43. Bhaskara S, Knutson SK, Jiang G, Chandrasekharan MB, Wilson AJ, Zheng S, Yenamandra A, Locke K, Yuan JL, Bonine-Summers AR, et al. Hdac3 is essential for the maintenance of chromatin structure and genome stability. *Cancer Cell* 2010;18:436–47.
 44. Zheng S, Li Q, Zhang Y, Balluff Z, Pan YX. Histone deacetylase 3 (HDAC3) participates in the transcriptional repression of the p16 (INK4a) gene in mammary gland of the female rat offspring exposed to an early-life high-fat diet. *Epigenetics* 2012;7:183–90.
 45. Gupta M, Han JJ, Stenson M, Wellik L, Witzig TE. Regulation of STAT3 by histone deacetylase-3 in diffuse large B-cell lymphoma: implications for therapy. *Leukemia* 2012;26:1356–64.
 46. Cheung KL, Kong AN. Molecular targets of dietary phenethyl isothiocyanate and sulforaphane for cancer chemoprevention. *AAPS J* 2010;12(1):87–97.
 47. World Health Organization. Cancer: cancer prevention. Date of acquisition: 29 October 2017; electronic data sheet available from: <http://www.who.int/cancer/prevention/en/>
 48. Ahuja D, Saenz-Robles MT, Pipas JM. SV40 large T antigen targets multiple cellular pathways to elicit cellular transformation. *Oncogene* 2005;24:7729–45.
 49. Keum Y-S, Yu S, Chang PP-J, Yuan X, Kim J-H, Xu C, Han J, Agarwal A, Kong A-NT. Mechanism of action of sulforaphane: inhibition of p38 mitogen-activated protein kinase isoforms contributing to the induction of antioxidant response element-mediated heme oxygenase-1 in human hepatoma HepG2 cells. *Cancer Res* 2006;66:8804–13.
 50. Morey SR, Smiraglia DJ, James SR, Yu J, Moser MT, Foster BA, Karpf AR. DNA methylation pathway alterations in an autochthonous murine model of prostate cancer. *Cancer Res* 2006;66:11659–67.
 51. Morey Kinney SR, Smiraglia DJ, James SR, Moser MT, Foster BA, Karpf AR. Stage-specific alterations of DNA methyltransferase expression, DNA hypermethylation, and DNA hypomethylation during prostate cancer progression in the transgenic adenocarcinoma of mouse prostate model. *Mol Cancer Res* 2008;6:1365–74.
 52. Horwitz GA, Zhang K, McBrien MA, Grunstein M, Kurdistani SK, Berk AJ. Adenovirus small e1a alters global patterns of histone modification. *Science* 2008;321:1084–5.
 53. Ali SH, DeCaprio JA. Cellular transformation by SV40 large T antigen: interaction with host proteins. *Semin Cancer Biol* 2001;11:15–23.
 54. Wang QS, Papanikolaou A, Nambiar PR, Rosenberg DW. Differential expression of p16(INK4a) in azoxymethane-induced mouse colon tumorigenesis. *Mol Carcinog* 2000;28:139–47.
 55. Romagosa C, Simonetti S, Lopez-Vicente L, Mazo A, Lleornart ME, Castellvi J, Ramon y Cajal S. p16(Ink4a) overexpression in cancer: a tumor suppressor gene associated with senescence and high-grade tumors. *Oncogene* 2011;30:2087–97.